Performance of ENVISAT ASAR for Operational Ocean Wind Field Retrieval

Jochen Horstmann and Wolfgang Koch

(1)GKSS Research Center
Max-Planck-Str. 1, D-21502 Geesthacht, Germany
Horstmann@gkss.de

INTRODUCTION

Today, several scatterometers (SCATs) are in orbit, which enable to measure wind fields with a resolution of up to 25 km on a global and operational basis independent on daylight and cloudiness. The SCATs were originally not designed to measure high resolution wind fields and therefore make it difficult to measure the highly spatially variable winds, which are especially important to measure in coastal areas. Since the launch of the European remote sensing satellites ERS-l, ERS-2 and ENVISAT as well as the Canadian satellite RADARSAT-1, synthetic aperture radar (SAR) images of the ocean surface with a resolution in the order of 10 m have been acquired on a continuous basis over the last 13 years. Their high resolution together with the large spatial coverage make them a valuable tool for measuring geophysical parameters such as ocean surface winds, waves, and sea ice. All the above mentioned SARs operate at C-band (5.3 GHz) with either vertical (VV) or horizontal (HH) polarization in transmit and receive at moderate incidence angles between 15° and 50°. For this electromagnetic wavelength and range of incidence angles the backscatter of the ocean surface is primarily caused by the small-scale surface roughness (in the range of 5 to 10 cm), which is strongly influenced by the local wind field and therefore allows the backscatter to be empirically related to the wind.

In this paper an algorithm for wind field retrieval from satellite borne SARs (WiSAR) operating at C-band with either VV- or HH-polarization is introduced. The algorithm is applied to retrieve wind fields from the advanced SAR (ASAR) aboard the ENVISAT satellite. To demonstrate the applicability of WiSAR, SAR retrieved wind fields are compared to results of a numerical atmospheric model.

UTILIZED SAR DATA

For the following investigations SAR data acquired by the European remote sensing satellite ENVISAT were used. ENVISAT operates in a Sun-synchronous polar orbit at a height of ~ 800 km with an orbital period of 100 min and a repeat cycle of 35 days. For this study the ENVISAT ASAR data were acquired in the ScanSAR wide swath mode. The ScanSAR images are generated by scanning the incidence angle and sequentially synthesizing images for different sub-swaths at incidence angles between 15° and 45°. In the ScanSAR wide swath mode ASAR can image a swath width of up to ~ 450 km with a spatial resolution of ~ 100 m. The ENVISAT ScanSAR data were acquired at C-band (5.34 GHz) with either HH- or VV-polarization

WIND DIRECTION RETRIEVAL

The most popular methods for SAR wind direction retrieval are based on the imaging of linear features at scales above 400 m, which are visible in SAR images. Most of these features are associated to wind streaks [1] and marine atmospheric boundary layer rolls [2]. Studies of Dankert et al. [3] utilizing high resolution real aperture radar (RAR) imagery have shown that wind induced streaks at scales between 50 to 1500 m are very well aligned with the mean surface wind. Their comparison of 3272 radar image sequences, acquired over a six month period, to *in situ* wind measurements showed that the streaks are very well aligned with the surface wind directions (root mean square error of 14.2° and bias of 0.6°). Therefore, in the following the linear features visible in the SAR images at short scales, typically below 3 km, are assumed to be aligned with the mean surface wind direction. The results of Dankert et al. [3] encourage to focus on the smallest resolved scales, which can be utilized from space borne SAR.

In the spatial domain the orientation of the streaks is derived by retrieving the local gradient at different scales [4 and 5]. In the following this method is referred as the Local Gradient Method (LG-Method). In the LG-Method the wind direction is defined as normal to the direction of the local gradient derived from smoothed amplitude images. In a first step the SAR images are smoothed and reduced to a pixel size of 100, 200 and 400 m, representing scales above 200 m. From these pixels the local directions, defined by the normal to the local gradient, are computed with a 180° ambiguity. In a next step all pixels that are effected by non wind induced features, e.g. land, surface slicks, sea ice etc. are masked. Therefore, land masks and SAR image filters, which are described by Koch [5], are applied. Finally, from all of the resulting directions only the most frequent directions in a predefined grid cell are selected. The wind directions resulting from the 100, 200 and 400 m pixel sizes vary typically only by a few degrees, except for cases were additional features are present in the SAR image, e.g. scalloping. The 180° directional ambiguity can be removed if wind shadowing is
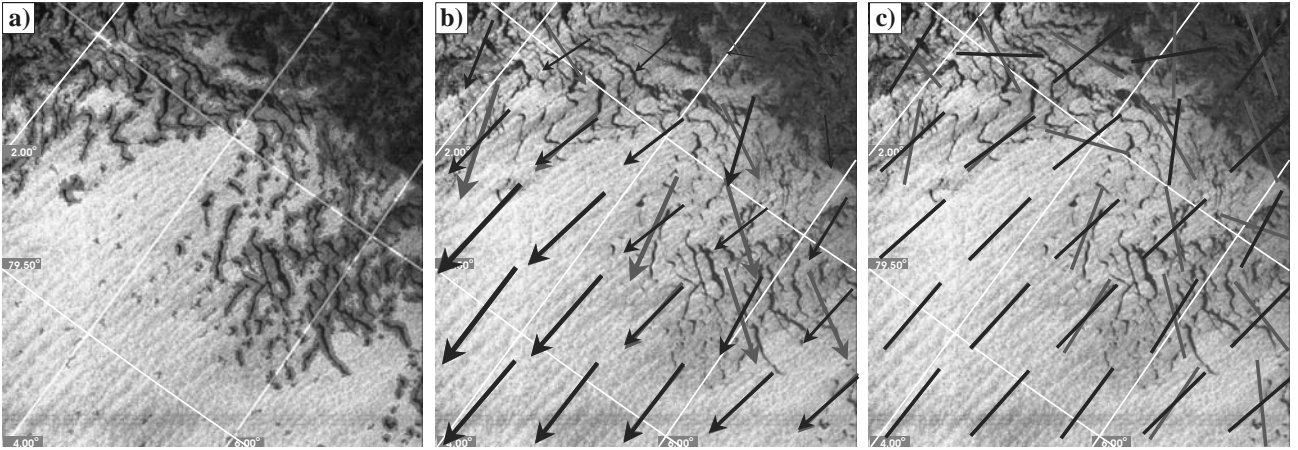
Fig. 1. ERS-1 SAR image acquired at the marginal ice zone off the coast of Spitzbergen. a) shows the mask superimosed to the SAR image, which results from the filtering. b) gives the wind directions resulting from the Local Gradient Method (LG-Method) with (dark grey arrows) and without (light grey arrows) consideration of the filter. c) shows the wind directions resulting from the Fast Fourier Transformation Method (FFT-Method) with (dark grey bars) and without (light grey bars) utilizing the filter.

present, which is often visible in the lee of coastlines. If such features are not present in the image other sources, e.g., atmospheric models or *in situ* measurements, have to be considered.

In Fig. 1 an ERS-1 SAR image is depicted, which was acquired at the marginal ice zone off the coast of Spitzbergen. In Fig. 1 a) the mask resulting from the filtering is superimposed to the SAR image. It is clearly visible that most pixels affected by sea ice are included in the masked area. In Fig. 1 b) the wind direction retrieved via the LG-Method are plotted with (dark grey arrows) and without (light grey arrows) the filter. It can be seen that the wind directions significantly improve utilizing the filter.

The most popular method for extraction of the wind direction from SAR imagery searches for the dominant wind streak direction in the spectral domain and is referred to as the Fast Fourier Transformation Method (FFT-Method). This method was first introduced by Gerling [6] and later modified by several other groups [7, 8, and 9]. In a first step all pixels in the SAR image that are effected by non wind induced features. Therefore a land mask and the filters, already used in the LG-Method, are applied to the image. In the next step the SAR image is split up into subimages, which represent the wind direction resolution that is typically set to 10 km x 10 km. Then all masked pixels in each subimge are replaced by the mean intensity value of the selected subimage, this enables to use the FFT-Method also close to the shore or at the marginal ice zone (Fig. 1 c)). In the last step a regression is estimated, weighted with the energy densities for wavelengths between 500 and 1800 m. The threshold of 500 m is set to exclude ocean surface waves, while the threshold of 1800 m is set to exclude larger scale features e.g. inflection point instabilities and Lee waves. The main spectral energy is located perpendicular to the orientation of the streaks, giving the wind direction with a 180° directional ambiguity. The 180° ambiguity can be removed if wind shadowing, e.g. in the Lee of the coast, or additional data e.g. wind forecasts are available.

WIND SPEED RETRIEVAL

For the wind speed retrieval a model function relating the NRCS of the ocean surface to the local near-surface wind speed, wind direction versus antenna look direction and incidence angle is utilized. This function is dependent on radar frequency and polarization. In case of the ERS-1 SCAT operating at C-band with VV polarization several empirical functions have been developed, of which the CMOD4 [10] and CMOD_IFR2 [11] are the most commonly used and the CMOD5 [12] is the most recently developed. It has been shown that these functions are applicable for wind speed retrieval from VV polarized SAR images [7, 9, and 13]. For wind speed retrieval from C-band HH polarized SAR images no similar well developed model exists so that a hybrid model function is applied that consists of the prior mentioned models, e.g. CMOD4, and a C-band polarization ratio (PR) [14, 15, and 16]. So far the PR is not well known and several different PR's are suggested in literature [17 and 18]. The PR proposed by Thompson et al. [18] neglects wind speed and wind direction dependency and is given by:

$$PR = \frac{(1 + \alpha \tan^2 \theta)^2}{(1 + 2 \tan^2 \theta)^2},$$

where α is a constant and set to 0.6, fitting the measurements of Unal et al. [19]. This form is closely related to theoretical forms of the PR. Several different values for α have been suggested in the past considering RADARSAT-1 SAR data, they vary between 0.4 and 1.2 [14, 16, and 20]. Comparisons of RADARSAT-1 SAR data of different SAR

processing facilities showed that the different findings of α are most likely due to the different calibrations of RADARSAT-1 SAR data.

COMPARISON

To validate WiSAR, which consists of the LG-Method and the CMOD4, and demonstrate WiSARs applicability for SAR wind field retrieval in the coastal zone several ENVISAT ScanSAR images of the North Sea were considered. From the 24 ENVISAT ScanSAR images 22 were acquired at VV polarization and 2 at HH polarization respectively. For the comparison in the North Sea wind fields from the model of the German Weather Service (DWD) were utilized, which represent 6 hour analyzed wind fields that were additionally interpolated to the ASAR acquisition time. The SAR wind fields were retrieved from the area corresponding to the grid cell in the DWD model output, resulting in an average grid cell size of approximately 45 km x 75 km. The directional ambiguities of the SAR-retrieved wind directions were removed by considering wind shadowing as well as weather charts. The resulting wind direction, mean NRCS, and mean incidence angle of each grid cell is taken as input to the wind speed retrieval algorithm for VV or HH polarization respectively. Fig. 2 (left hand side) shows an ENVISAT ASAR image of the southern North Sea acquired on December 14, 2002, at 09:53 UTC in the ScanSAR mode with HH polarization. Superimposed to the image are the wind vectors as retrieved from the SAR image using WiSAR (white arrows) and resulting from the DWD model (grey arrows). The wind direction ambiguities could be removed due to the wind shadowing, which is especially visible at the east coast of the German coast. The contrast enhanced cutout (lower right of Fig. 2 left hand side) shows the wind shadowing in more detail, especially in Lee of the island Sylt. In most parts of the image the SAR retrieved winds agree very well to the DWD model results both in magnitude and direction. Fig. 2 right hand side shows an ENVISAT ASAR image of the southern North Sea acquired on June 20, 2003, at 21:09 UTC. In this case the image was acquired in VV polarization. Again the wind fields resulting from the SAR image and the DWD model agree very well. In the upper right of Fig. 2 a cutout is shown of the SAR retrieved wind field at a resolution of 10 km, which shows the smaller scale variability of the wind field.

Concerning the comparison of wind directions resulting from the DWD model to those retrieved from the ENVISAT ASAR images the LG-Method showed significantly better results than the FFT-method [21]. The FFT-Method is strongly affected by scalloping, which is often visible in RADARSAT and ENVISAT ScanSAR images. Scalloping is a processing problem, which leads to linear streak like features that are aligned in range direction with a spacing within the scales evaluated by the FFT-Method and can therefore lead to a misinterpretation of wind directions [4]. In case of
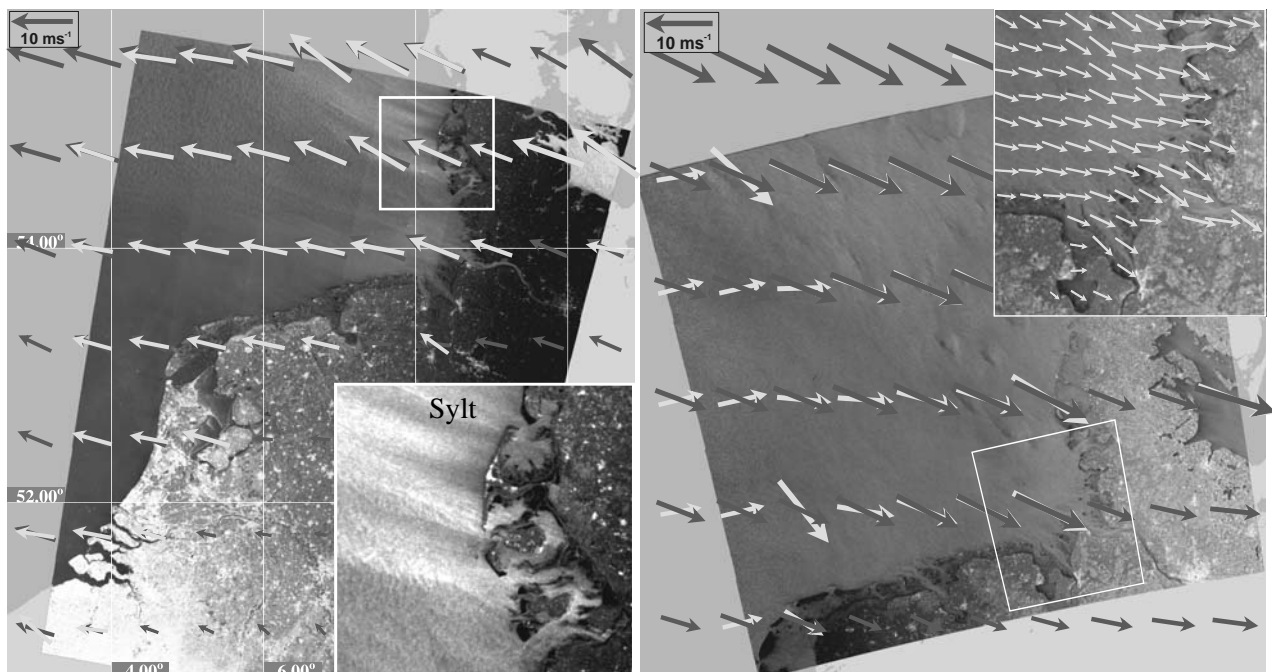

Fig. 2. ENVISAT ASAR images of the southern North Sea acquired on 14. December, 2002 with HH polarization (left hand side) and on 20. June, 2003 with VV polarization (right hand side). Superimposed to the images are the wind vectors resulting from the SAR data using WiSAR(white arrows) and from the model of the German weather service (grey arrows). The contrast enhanced cutout of the left hand side image shows the wind shadowing due to the coast, which is used to remove the directional ambiguity. The cut out on the right hand side shows the SAR wind field retrieved at a higher resolution (10 km).

the LG-Method scalloping only affects the reduced pixel sizes below 400 m, which enables the algorithm to overcome this handicap. In the following all SAR retrieved winds were derived using as input to the C-band model the wind directions resulting from the LG-Method.

The comparison considering all 24 ENVISAT ScanSAR images is shown in Fig. 3, which includes 709 co-locations to the DWD model results. In Fig. 3. (left hand side) wind directions from the DWD model are plotted versus the wind directions resulting from the ScanSAR data. The main statistical parameters are: correlation of 0.95, bias of -0.2° and a root mean square error of 18.9°. These results are very promising especially if compared to the wind direction error of 15° achieved by the SCAT aboard ERS [11]. On the right hand side of Fig. 3 the wind speeds from the DWD model are plotted versus the wind speeds resulting from the ScanSAR data. The main statistical parameters are: correlation of 0.82, bias of -0.1 ms^{-1} and a root mean square error of 2.3 ms^{-1}. The comparison of SAR retrieved wind speeds to the model results do not show a good consistency, which is most likely due to the scarce resolution of the atmospheric models, which is too coarse for resolving wind shadowing as well as other small scale features that occur especially near to the coasts. Similar results were obtained when comparing RADARSAT-1 ScanSAR retrieved wind fields to numerical model results at the coasts of Greenland [4].

Comparisons of wind speeds off the coasts were obtained by Horstmann et al. [13]. They retrieved from a global ERS-2 SAR imagette (10 km x 10 km SAR images aquired in the SAR wave mode) data set the wind speeds and compared them to results of the ERS-2 SCAT and the numerical model of the European Center for Medium-range Weather Forecast (ECMWF). SAR imagettes are typically acquired off the coasts and therefore the wind field is not effected by land, e.g., wind shadowing. Three weeks of ERS-2 SAR imagettes, representing a total of 34000 SAR imagettes were utilized. Overall the agreement to both ECMWF (1.6 ms^{-1}) and ERS-2 SCAT (1.0 ms^{-1}) results is excellent and agrees well to the error of 1.3 ms^{-1} reported for ERS-2 SCAT wind speeds.
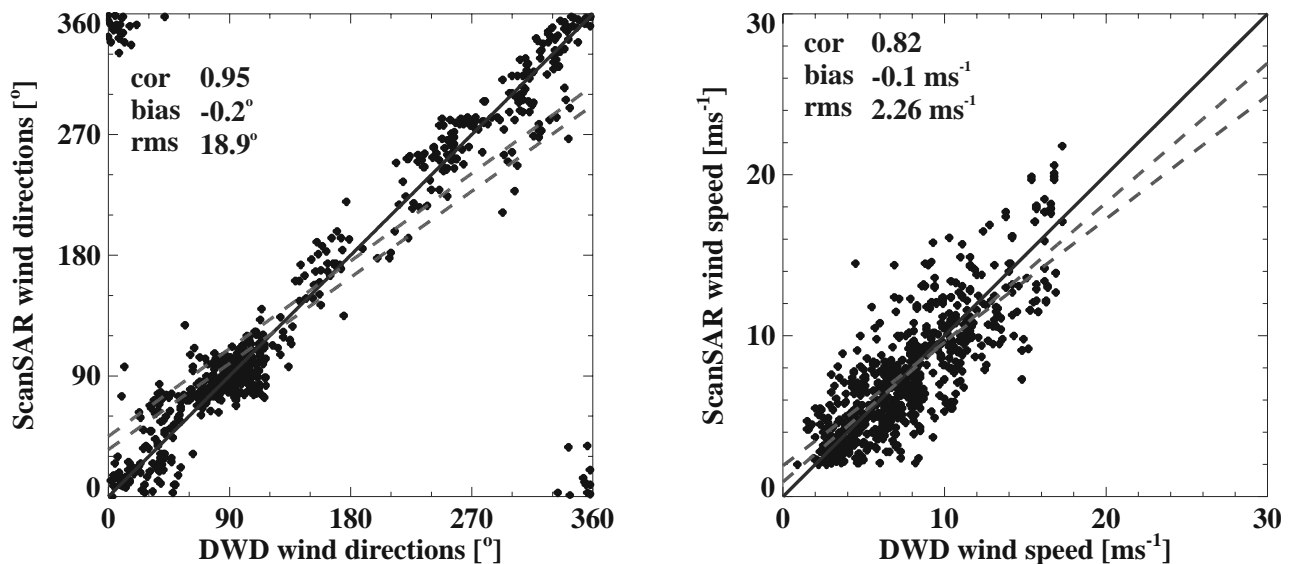

Fig. 3. Comparison of DWD model winds to ENVISAT ASAR retrieved winds. On the left hand side the wind direction comparison is shown were the SAR wind directions were retrieved using the LG-Method. On the right hand side the wind speed comparison is shown using the CMOD4 model.

CONLUSIONS

Two methods the LG- and FFT-Method for retrieving wind directions have been developed. The LG-Method retrieves the orientation of the wind streaks in the spatial domain considering the local gradients at a grid cell size of 100, 200 and 400 m. The FFT-Method extracts the wind direction in the spectral domain searching for the dominant spectral peak at wave lengths between 500 and 1800 m. Both methods work significantly better if filters for excluding non wind induced features are applied. Comparison of SAR retrieved wind directions using WiSAR, to the DWD model analysis resulted in a root mean square error of 18.8° with a negligible bias. For wind speed retrieval WiSAR utilizes the C-band model CMOD4, which was developed for the VV polarized C-band scatterometers aboard ERS. In case of HH polarization the CMOD4 was extended by an incidence angle dependent polarization ratio. As input to the CMOD4 the NRCS, incidence angle and wind direction is needed, which can be retrieved from the SAR image. Comparison of SAR retrieved wind speeds to DWD model analysis resulted in a standard deviation of 2.3 ms^{-1} and a negligible bias. Considering SAR data acquired well off the coast showed a wind speed error of 1.0 ms^{-1}. It is very likely that the large wind speed error in the ENVISAT ScanSAR comparison is due to the atmospheric model, which is too coarse for resolving wind shadowing as well as other small scale features that occur especially near to the coasts. The overall good

agreement of SAR retrieved wind fields to model and SCAT results shows the applicability of WiSAR for ocean surface wind retrieval from C-band SAR data. The obtained SAR wind retrieval errors are in the same magnitude as the results achieved by satellite borne SCATs.

Future investigations will have to concentrate on the validity of the C-band models, especially concerning high wind speeds and polarization. Concerning the wind direction retrieval from wind induced streaks, it has to be investigated which scales are the most appropriate to infer on the ocean surface wind direction.

ACKNOWLEDGMENTS

REFERENCES

[1] P. Drobinski and R.C. Foster, On the Origin of Near-Surface Streaks in the Neutrally-Stratified Planetary Boundary Layer, *Bound.-Layer Meteorol.,* vol. 108(2), p. 247-256, 2003.

[2] W. Alpers and B. Brümmer, Atmospheric Boundary Layer Rolls Observed by the Synthetic Aperture Radar Aboard the ERS-1 Satellite, *J. Geophys. Res.,* vol. 99, p. 12 613-12 621, 1994.

[3] H. Dankert, J. Horstmann, and W. Rosenthal, Ocean Wind Fields Retrieved from Radar-Image Sequences, *J. Geophys. Res.*, vol. 108(C11), 3352, doi: 10.1029/2003JC002056, 2003.

[4] J. Horstmann, W. Koch, S. Lehner, and R. Tonboe, Ocean Winds from RADARSAT-1 ScanSAR, *Can. J. Remote Sens.*, vol. 28(3), p. 524-533, 2002

[5] W. Koch, Directional Analysis of SAR Images Aiming at Wind Direction, *IEEE Trans. Geosci. Remote Sens.*, 2004.

[6] T.G. Gerling, Structure of the Surface Wind Field from Seasat SAR, *J. Geophys. Res.*, vol 91, p. 2308-2320, 1986.

[7] P. W. Vachon and F.W. Dobson, Validation of Wind Vector Retrieval from ERS-1 SAR Images over the Ocean, *Global Atmos. Ocean Syst.*, vol. 5, p. 177-187, 1996.

[8] C.C. Wackerman, C.L. Rufenach, R. Schuchman, J.A. Johannessen, and K. Davidson, Wind Vector Retrieval using ERS-1 Synthetic Aperture Radar Imagery, *J. Geophys. Res.,* vol. 34, p 1343-1352, 1996.

[9] S. Lehner, J. Horstmann, W. Koch, and W. Rosenthal, Mesoscale Wind Measurements using Recalibrated ERS SAR Images, *J. Geophys. Res.*, vol. 103, p. 7847-7856, 1998.

[10] A. Stoffelen and D. Anderson, Scatterometer Data Interpretation: Estimation and Validation of the Transfer Function CMOD4, *J. Geophys. Res.*, vol. 102, p. 5767-5780, 1997.

[11] Y. Quilfen, B. Chapron, T. Elfouhaily, K. Katsaros, and J. Tournadre, Observation of Tropical Cyclones by High-Resolution Scatterometry, *J. Geophys. Res.*, vol. 103, p. 7767-7786, 1998.

[12] H. Hersbach, CMOD5 an Improved Geophysical Model Function for ERS C-band Scatterometry, *Internal Report: European Centre for Medium-Range Weather Forecast*, 2003.

[13] J. Horstmann, H. Schiller, J. Schulz-Stellenfleth, and S. Lehner, Global Wind Speed Retrieval from SAR, *IEEE Trans. Geosci. Remote Sens.*, vol. 41(10), p. 2277-2286, 2003.

[14] J. Horstmann, W. Koch, S. Lehner, and R. Tonboe, Wind Retrieval over the Ocean using Synthetic Aperture Radar with C-band HH Polarization, *IEEE Trans. Geosci. Remote Sens.*, vol. 38(5), p. 2122-2131, 2000.

[15] D.R. Thompson and R.C. Beal, Mapping of Mesoscale and Submesocale Wind Fields using Synthetic Aperture Radar, *John Hopkins APL Tech. Dig.*, vol. 21(1), p. 58-67, 2000.

[16] P.W. Vachon and F.W. Dobson, Wind Retrieval from RADARSAT SAR Images: Selection of a Suitable C-band HH Polarization Wind Retrieval Model, *Can. J. Remote Sens.*, vol. 26(4), p. 306-313, 2000.

[17] T. Elfouhaily, Physical Modeling of Electromagnetic Backscatter from the Oean Surface; Application to Retrieval of Wind Fields and Wind Stress by Remote Sensing of the Marine Atmospheric Boundary Layer, *Travail de recherche effectué au sein Département d'Océanographie Spatiale de l'Institut Francais de Recherche pour l'Exploitation de la Mer (IFREMER)*, Brest, France, 1997.

[18] D.R. Thompson, T.M. Elfouhaily, and B. Chapron, Polarization Ratio for Microwave Backscattering from the Ocean Surface at Low to Moderate Incidence Angles, Proc. *Int. Geosci. Remote Sens. Symp.,* Seattle, USA, 1998.

[19] C.M.H. Unal, P. Snoeij, and P.J.F. Swart, The Polarization-dependent Relation Between Radar Backscatter from the Ocean Surface and Surface Wind Vectors at Frequencies Between 1 and 18 GHz, *IEEE Trans. Geosci. Remote Sens.*, vol. 29, p. 621-626, 1991.

[20] F. Monaldo, D. Thompson, R. Beal, W. Pichel, and P. Clemente-Colon, Comparison of SAR-derived Wind Speed with Model Predictions and Ocean Buoy Measurements, *IEEE Trans. Geosci. Remote Sens.,* vol. 39(12), p. 2587-2600, 2002.

[21] J. Horstmann and W. Koch, High Resolution Ocean Surface Wind Fields Retrieved from Spaceborne Synthetic Aperture Radars Operating at C-Band, ESA SP-Series, submitted 2004.